

Rapid Movement of Microtubules in Axons

Lei Wang¹ and Anthony Brown^{2,3}

¹Graduate Program in Biological Sciences
Ohio University
Athens, Ohio 45701

²Neurobiotechnology Center and
Department of Neuroscience
The Ohio State University
Columbus, Ohio 43210

Summary

Cytoskeletal and cytosolic proteins are transported along axons in the slow components of axonal transport at average rates of about 0.002–0.1 $\mu\text{m/s}$. This movement is essential for axonal growth and survival, yet the mechanism is poorly understood. Many studies on slow axonal transport have focused on tubulin, the subunit protein of microtubules, but attempts to observe the movement of this protein in cultured nerve cells have been largely unsuccessful. Here, we report direct observations of the movement of microtubules in cultured nerve cells using a modified fluorescence photobleaching strategy combined with difference imaging. The movements are rapid, with average rates of 1 $\mu\text{m/s}$, but they are also infrequent and highly asynchronous. These observations indicate that microtubules are propelled along axons by fast motors. We propose that the overall rate of movement is slow because the microtubules spend only a small proportion of their time moving. The rapid, infrequent, and highly asynchronous nature of the movement may explain why the axonal transport of tubulin has eluded detection in so many other studies.

Introduction

The slow axonal transport of tubulin has attracted intense interest and controversy for more than 10 years [1–4]. The principal reason for this has been the failure of numerous attempts to demonstrate the movement of fluorescently labeled tubulin in axons by using fluorescence photobleaching and photoactivation approaches [5–9]. Bulk movement of axonal microtubules has been observed by using these techniques in neurons cultured from *Xenopus* embryos [10–12], but this appears to have been due to stretching of the axons during their growth on laminin substrates rather than bona fide axonal transport [11, 13]. Direct observation of fluorescently labeled tubulin has revealed the movement of individual microtubules in growth cones and nascent axonal branches [14, 15], but attempts to observe such movements in axons by using fluorescence speckle microscopy have been unsuccessful [16].

Recent observations on the movement of neurofilament proteins in axons indicate that the movements in

slow axonal transport may actually be fast and asynchronous and that the overall rate is slow because the rapid movements are interrupted by prolonged pauses [17–19]. If tubulin is transported along axons in this manner, why did previous studies not detect this movement? One possible explanation is that the rapid intermittent movements went unnoticed in those studies because the experiments were designed with the expectation of a slow and synchronous movement. For example, previous photobleaching studies all used short bleached regions (about 3 μm long) and long time-lapse intervals (5 min or more) [5–9, 12, 13]. In support of this hypothesis, we have recently shown that the axonal transport of neurofilaments can be detected by fluorescence photobleaching if the bleaching strategy is optimized to detect rapid asynchronous movements [20]. Here, we show that this modified bleaching strategy, in combination with difference imaging, can also reveal the movement of microtubules in axons. Our data indicate that the microtubules are transported by fast motors. We propose that the rapid, infrequent, and asynchronous movement of these cytoskeletal polymers can explain why their movement was not detected in previous studies.

Results and Discussion

To visualize tubulin in axons, we injected rhodamine-labeled tubulin into the cell bodies of cultured rat sympathetic neurons 2–5 hr after plating and then observed the cells 2–24 hr later. To determine the extent of the incorporation of the rhodamine-labeled tubulin into microtubules, we visualized axonal microtubules by immunofluorescence microscopy of splayed axonal cytoskeletons 18–20 hr after injection (Figure 1). Rhodamine fluorescence was present along 91% of the total microtubule length (data pooled from splayed regions of 15 different cells; total length measured 1953 μm). To quantify the proportion of the fluorescent tubulin that assembled into polymers, we permeabilized neurons with 0.5% saponin under conditions that preserve the integrity of the axonal microtubule bundle (see the Experimental Procedures). The proportion of the rhodamine fluorescence that remained in the permeabilized axons was $78\% \pm 0.7\%$ (mean \pm SD, $n = 5$), which is consistent with the results of biochemical studies on the extent of tubulin polymerization in these neurons [21]. These data indicate that the rhodamine-labeled tubulin was assembly competent and that it equilibrated with the endogenous tubulin pool.

To detect the axonal transport of rhodamine-labeled tubulin, we bleached the rhodamine fluorescence in long regions of axon (15–70 μm in length; Figure 2) and then observed the bleached regions by time-lapse imaging. In no case did the entire bleached region move. This is consistent with the results of previous photobleaching studies on tubulin in cultured neurons [5–9, 12, 13], and it confirms that tubulin is not transported in a slow and

³Correspondence: brown.2302@osu.edu

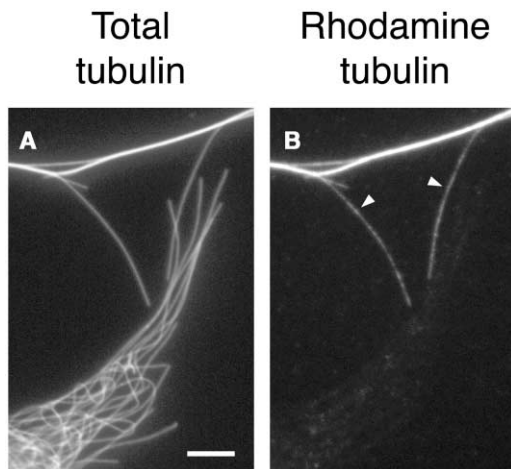


Figure 1. Assembly of Fluorescent Tubulin into Microtubules
Image of splayed axonal microtubules (white arrowheads) showing the incorporation of rhodamine-labeled tubulin along their length. The neuron was injected with rhodamine tubulin and then extracted with 1% Triton X-100, which causes some of the microtubules to splay apart from the axon (see the Experimental Procedures). Below the axon is a nonneuronal cell that was not injected with rhodamine-labeled tubulin.
(A) Total tubulin visualized by immunofluorescence microscopy with a monoclonal antibody specific for β -tubulin and a fluorescein-conjugated secondary antibody.
(B) Rhodamine-labeled tubulin visualized directly, without the use of antibodies. The scale bar represents 5 μm .

synchronous manner. To detect rapid asynchronous movements, we acquired time-lapse images at short time intervals (2–4 s). Under these conditions, we observed rapid but infrequent movement of short microtubules through the bleached regions. These microtubules were fluorescent because they originated from the unbleached regions of axon that flanked the bleached regions. Nevertheless, detection of these microtubules was challenging because the pool of unpolymerized tubulin rapidly recovered its fluorescence after photobleaching due to the diffusion of fluorescent tubulin from the adjacent unbleached regions. In most axons, this fluorescence was sufficient to completely or partially obscure the moving polymers. To address this problem, we limited our studies to thin axons, which we were able

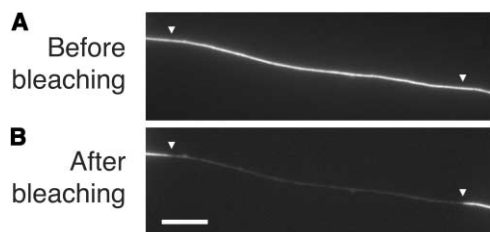


Figure 2. Fluorescence Photobleaching
(A) A fluorescent axon prior to photobleaching.
(B) The same axon after photobleaching by continuous excitation of the fluorescence for 120 s (see the Experimental Procedures). The white arrowheads mark the proximal and distal ends of the bleached region, which measured 63 μm in length. The scale bar represents 10 μm .

to bleach more extensively. In addition, we performed difference imaging on the time-lapse movies to improve our ability to detect movement (see Figure 3 and two movies in the Supplementary Material available with this article online).

To analyze the movement, we recorded time-lapse movies of 54 bleached axons from 22 cells. The duration of the movies ranged from 2.5 to 10 min. The microtubules ranged in length from 1.1 to 5.0 μm (average = 2.7 μm , $n = 71$; Figure 4C), but we cannot exclude the possibility that the tubulin also moved in a punctate form that was too faint to detect with our present approach. Figure 4A shows the motile behavior of six representative microtubules. The microtubules moved rapidly, but the movements were often interrupted by prolonged pauses. The bouts of movement often persisted for many tens of micrometers, and the transitions between the moving and pausing states were often abrupt. The movements were also infrequent and bidirectional. On average, we observed one microtubule move through the bleached gaps every 4.2 min, and 87% moved in a net anterograde direction. Some of the microtubules exhibited brief reversals of direction (Figure 4A), but sustained reversals were relatively rare. For example, we only observed three reversals that were sustained for a duration of more than 25 s or a distance of more than 15 μm .

For the 78 microtubules that we tracked, the average time spent pausing was 54%, but this is likely to be an underestimate for the entire microtubule population because we were not able to track microtubules that paused throughout the observation period. The average velocity, excluding pauses, for the microtubules that moved, ranged from 0.24 to 2.89 $\mu\text{m/s}$ in the anterograde direction (average = 1.01 $\mu\text{m/s}$, $n = 68$) and from 0.36 to 1.87 $\mu\text{m/s}$ in the retrograde direction (average = 1.06 $\mu\text{m/s}$, $n = 10$; Figure 4B). The net average velocity for all the moving microtubules, excluding pauses (considering anterograde velocities as positive and retrograde velocities as negative), was 0.67 $\mu\text{m/s}$ in the anterograde direction. The peak velocities ranged from 0.42 to 4.17 $\mu\text{m/s}$ in the anterograde direction (average = 2.03 $\mu\text{m/s}$, $n = 68$) and from 0.89 to 2.92 $\mu\text{m/s}$ in the retrograde direction (average = 1.92 $\mu\text{m/s}$, $n = 10$; Figure 4B).

These data indicate that fluorescence photobleaching can reveal movement of tubulin in axons if the experimental strategy is designed to detect rapid infrequent movements of microtubules. The movements described here are too rapid to be accounted for by microtubule treadmilling because even the most rapid rates of treadmilling *in vivo* do not exceed 0.02 $\mu\text{m/s}$ [22]. Moreover, we have observed equally rapid rates of movement in the presence of 50 nM vinblastine (net average velocity = 1.05 $\mu\text{m/s}$ in the anterograde direction, average peak velocity = 1.82 $\mu\text{m/s}$ in the anterograde direction, $n = 21$; data not shown), which is a condition that is known to suppress microtubule dynamics in cultured rat sympathetic neurons [23].

The rapid, infrequent, and highly asynchronous movements of microtubules reported here are similar to those that we and others have observed for neurofilaments [17, 18, 20], with some notable differences. One difference is that the microtubules moved more rapidly (aver-

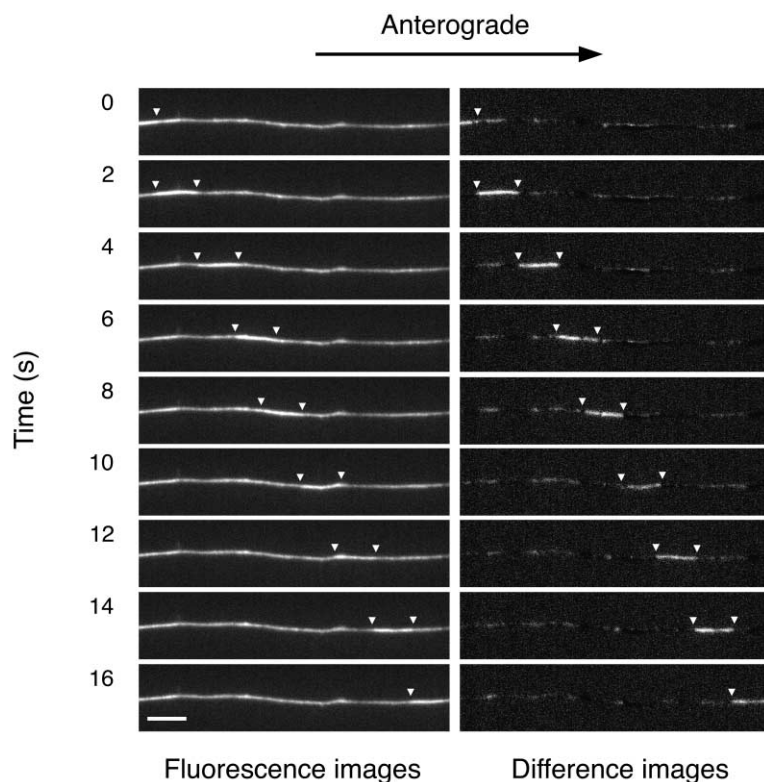


Figure 3. Movement of a Microtubule in a Photobleached Axon

Time-lapse images of a microtubule moving in an anterograde direction through the photobleached region of an axon. The images were acquired at 2-s intervals without pixel binning. The edges of the photobleached region are outside the field of view. The images on the left represent the raw, unprocessed fluorescence images, and the images on the right represent the corresponding difference images (see the Experimental Procedures). White arrowheads mark the leading and trailing ends of the microtubule, which measured 5 μm in length and moved rapidly through the photobleached region at an average velocity of 2.49 $\mu\text{m}/\text{s}$. The microtubule is barely visible above the background of fluorescent tubulin in the raw images, but it can be seen clearly in the difference images. Proximal is oriented toward the left, and distal is oriented toward the right. The scale bar represents 5 μm . The original movie (Movie 1) can be viewed in the Supplementary Material (time compression 15:1).

age velocity of $\approx 1 \mu\text{m}/\text{s}$ compared to $\approx 0.5 \mu\text{m}/\text{s}$ for neurofilaments) and spent a smaller proportion of their time pausing ($\approx 50\%$ compared to $\approx 70\%$ for neurofilaments) [20]. This is consistent with radioisotopic pulse-labeling studies, which have shown that neurofilaments move exclusively in the slower subcomponent of slow axonal transport, termed Slow Component “a”, whereas, in many neurons, a proportion of the tubulin moves in Slow Component “b”, which is approximately 5–10 times faster [24, 25]. Another difference is that the moving microtubules were also somewhat shorter and more uniform in length than the moving neurofilaments. For example, the average neurofilament length in our most recent study was 4.5 μm (range = 0.7–15.8 μm , $n = 64$) [20], whereas the average microtubule length in the present study was 2.7 μm (range = 1.1–5.0 μm , $n = 71$). The short length of the moving neurofilaments and microtubules is noteworthy because it is our impression that the average neurofilament and microtubule length in these neurons is considerably greater, and it is clear that many neurofilaments and microtubules in cultured neurons attain lengths in excess of 100 μm [26–28]. This suggests the intriguing possibility that severing mechanisms may be a necessary prerequisite for the movement of neurofilaments and microtubules in axons. In this regard, it is interesting that katanin, a microtubule-severing protein, is distributed throughout the axon and that its severing activity is required for axon growth, though its function in axons has yet to be determined [29].

In recent years, a variety of approaches in cultured neurons have provided indirect evidence that axonal microtubules are nucleated at the neuronal centrosome and then transported out along the axon in the form of

assembled polymers [23, 30–32]. In contrast, observations on the bulk movement of fluorescent tubulin in squid axons have led others to conclude that axonal microtubules are stationary and that tubulin moves in the form of free subunits or small oligomeric assemblies [33, 34]. The present data directly demonstrate the movement of microtubules in axons of cultured neurons, and this supports the hypothesis that microtubules are cargo structures for the axonal transport of tubulin. The microtubules move rapidly, but the overall rate of movement is likely to be considerably slower because the movements are also very infrequent. Thus, it appears that both microtubules and neurofilaments move rapidly but intermittently, and that these polymers may actually spend most of their time pausing during their journey along the axon. This surprising motile behavior may explain why the axonal transport of tubulin and other cytoskeletal and cytosolic proteins is so slow, and why this movement has eluded direct observation for so many years.

The rapid bidirectional movement of microtubules in axons indicates that they are propelled by fast motors, similar in their mechanochemistry to the motors that move membranous organelles in the fast components of axonal transport [35]. Since axonal microtubules are all orientated with their plus ends distal, it is most likely that the anterograde and retrograde movements are generated by motor proteins of opposing directionality. By analogy with other forms of intracellular motility, these motors are likely to move the microtubules relative to a substrate against which they generate force. One category of potential mechanisms would involve the interaction of the moving microtubules with the head domains of microtu-

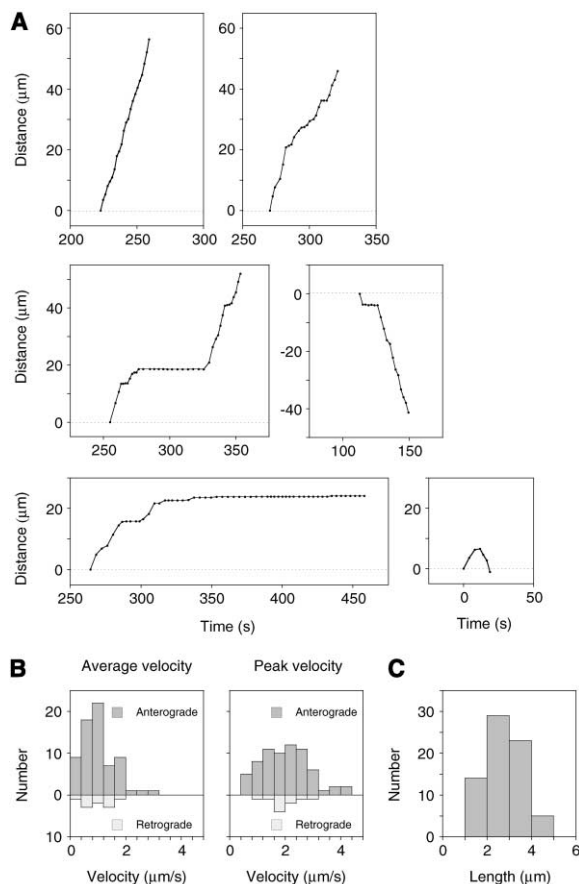


Figure 4. Analysis of Moving Microtubules

(A) Movements of four anterogradely moving microtubules, one retrogradely moving microtubule, and one microtubule that reversed direction. Each point represents the distance of the microtubule from the starting position, measured along the axon. Anterograde and retrograde movements are represented as positive and negative displacements, respectively. The abscissa represents the time elapsed since the start of the movie. In some cases, the acquisition interval was altered during the observation period (see Experimental Procedures), which explains why the spacing between the points varies in some of the traces.

(B) Histograms of average velocities (excluding pauses) and peak velocities for 78 microtubules.

(C) Histogram of lengths for 70 microtubules.

bule motors whose tail domains are anchored to other cytoskeletal polymers. The resulting movement would be analogous to microtubule gliding on glass coverslips coated with microtubule motor proteins. For example, dynein could generate anterograde movement by processing toward the minus ends of the moving microtubules [36]. In support of this hypothesis, inhibition of dynein function blocks the entry of microtubules into axons in cultured neurons [37]. Another category of potential mechanisms would involve short microtubules binding to the cargo binding domains of microtubule motor proteins and translocating along longer microtubules. For example, in this scenario, anterograde movement could be accomplished by a novel plus end-directed kinesin capable of binding to microtubules via its cargo binding domain, thereby generating sliding forces between two microtubules of the same orientation.

Experimental Procedures

Cell Culture

Neurons dissociated from the superior cervical ganglia of neonatal (P0–P1) rats were plated onto glass coverslips coated with poly-D-lysine (Sigma, M_w 70–150,000) and either Matrigel or laminin (Collaborative Research, 10 $\mu\text{g/ml}$). Cultures were maintained at 37°C in Liebovitz's L-15 medium (GIBCO Life Technologies; phenol red-free) supplemented with 0.6% glucose, 2 mM L-glutamine, 100 ng/ml 2.5S nerve growth factor (Collaborative Research), 10% adult rat serum, and 0.5% hydroxypropylmethylcellulose (Methocel, Dow Corning).

Microinjection

Rhodamine-labeled bovine brain tubulin was purchased from Cytoskeleton as a lyophilized powder and was reconstituted at a concentration of 10 mg/ml in a buffer composed of 50 mM potassium glutamate and 1 mM MgCl_2 (pH 7.0). The fluorescent tubulin was injected into the cytoplasm of neuronal cell bodies with a 3-axis hydraulic micromanipulator (Narashige) and a pressure injector (Medical Systems Corporation).

Immunofluorescence Microscopy and Detergent Extraction

To determine the proportion of the fluorescent tubulin in polymers, cells were permeabilized with 0.5% saponin in a microtubule-stabilizing buffer composed of 10 μM paclitaxel (Molecular Probes), 0.1% DMSO, 60 mM NaPIPES, 25 mM NaHEPES, 10 mM NaEGTA, and 2 mM MgCl_2 (pH 6.9), and the fluorescence intensity was quantified in the axons before and after permeabilization, as described previously [38]. Splayed axonal cytoskeletons were produced by extracting neurons with 1% Triton X-100 and 0.2 M NaCl in microtubule-stabilizing buffer (see above). We have shown previously that these conditions cause the axonal microtubules to splay apart from each other and adhere to the glass coverslip, allowing individual axonal microtubules to be resolved by fluorescence microscopy [26]. The splayed microtubules were fixed with a mixture of 4% formaldehyde and 0.5% glutaraldehyde and were processed for immunofluorescence microscopy by using a monoclonal antibody specific for β -tubulin (Amersham Pharmacia) as described previously [26].

Live-Cell Imaging

For live-cell imaging, cells were enclosed in a sealed chamber containing oxygen-depleted culture medium as previously described [17] and were observed by epifluorescence and differential interference contrast microscopy with a Nikon Diaphot 300 inverted microscope. Photobleaching and image acquisition were performed with a Nikon 100 \times /1.4NA Plan Apo oil immersion objective and a TRITC filter set (Chroma Technology, HQ 41002b). The temperature on the microscope stage was maintained at approximately 35°C by using a Nicholson ASI-400 Air Stream Incubator (Nevtek). For time-lapse imaging, the epifluorescent illumination was attenuated by 70%–90% by using neutral density filters, and images were acquired at 1.5- to 4-s intervals with 0.2- to 1-s exposures by using MetaMorph software (Universal Imaging) and a Quantix cooled CCD camera equipped with a Kodak KAF1400 chip (Roper Scientific). The camera was operated at maximum gain with a readout rate of 5 MHz. To maximize the signal-to-noise ratio, most images were acquired with 2 \times 2 pixel binning. The delay between the end of the photobleaching and the start of the time-lapse imaging was typically less than 1 min and was never more than 3.6 min. Because of the rapid and infrequent nature of the movements, we often set the default time-lapse interval to 4 s in the Acquire Time-lapse dialog box of the MetaMorph software and then acquired images more frequently by manually triggering image acquisition at shorter intervals when movements were observed. For the vinblastine experiments, neurons were treated with 50 nM vinblastine sulfate (Sigma) in culture medium for 1–2 hr prior to imaging [23].

Photobleaching

For bleaching, the fluorescent tubulin was excited by continuous unattenuated illumination with the 100 W mercury arc lamp for 60–120 s (average = 105 s, $n = 54$) as described previously [20] with the TRITC filter set. The radiance of the illumination at the specimen

plane was 600 kW/m² (measured with a LI-190SA Quantum Sensor, LI-COR). The size of the photobleached region was adjusted with the field aperture diaphragm in the epifluorescence illumination light path. Bleaching was performed on thin axons, which were generally located in distal portions of the axonal arbor, approximately 80–300 μm from the growth cone. The number of regions bleached per neuron ranged from one to nine (average = 2.5), but we never bleached more than one region within the same axonal branch (i.e., multiple bleached regions within a single cell were separated from each other by at least one major branch point). Inspection of the axons by differential interference microscopy did not reveal any alteration in axonal morphology or refractivity associated with the photobleaching process.

Image Processing and Analysis

Motion analysis was performed by tracking the position of the leading or trailing ends of the microtubules in successive time-lapse image frames by using the TrackPoints drop-in module of the MetaMorph software. We analyzed all fluorescent structures that could be tracked unambiguously and that exhibited a net displacement of at least ten pixels (1.37 μm) during the observation period. Pausing was defined as a movement of less than 0.0685 μm/s (one pixel per second at a binning factor of 1), which represents the precision limit of our measurements [17]. To facilitate the detection and analysis of the microtubules, we often performed difference imaging by subtracting the image immediately preceding the sequence of interest from each frame in that sequence. This procedure selectively revealed increases and decreases in the fluorescence intensity such as those associated with the movement of structures in the axon, and it allowed us to detect movements that might otherwise have been obscured by the fluorescence of other microtubules and tubulin subunits. Microtubule lengths were measured by manually tracing the axis of the polymer in a single frame. Because of the rapid rate of movement, there was some blurring of the moving microtubules within each image during the camera exposure. To control for any effect of this blurring on our length measurements, we measured microtubule lengths during phases of movement and pausing and determined the relationship between length and rate of movement for each microtubule by linear regression analysis. The average overestimation of length was 0.24 μm per μm/s ($R = 0.50$, $n = 61$). Based on the lengths and velocities of the moving microtubules, we calculate that our measurements overestimated the actual microtubule length by an average of 10% ± 8% (mean ± SD, $n = 61$).

Supplementary Material

Supplementary Material in the form of two QuickTime movies is available at <http://images.cellpress.com/supmat/supmatin.htm>.

Acknowledgments

This work was funded by a grant from the National Institute of Neurological Disorders and Stroke to A.B.

Received: June 5, 2002

Revised: July 4, 2002

Accepted: July 4, 2002

Published: September 3, 2002

References

1. Baas, P.W., and Brown, A. (1997). Slow axonal transport: the polymer transport model. *Trends Cell Biol.* 7, 380–384.
2. Hirokawa, N., Terada, S., Funakoshi, T., and Takeda, S. (1997). Slow axonal transport: the subunit transport model. *Trends Cell Biol.* 7, 384–388.
3. Hollenbeck, P.J., and Bamberg, J.R. (1999). Axonal microtubules stay put. *Nat. Cell Biol.* 1, E171–E173.
4. Shah, J.V., and Cleveland, D.W. (2002). Slow axonal transport: fast motors in the slow lane. *Curr. Opin. Cell Biol.* 14, 58–62.
5. Lim, S.-S., Sammak, P.J., and Borisy, G.G. (1989). Progressive and spatially differentiated stability of microtubules in developing neuronal cells. *J. Cell Biol.* 109, 253–263.
6. Lim, S.-S., Edson, K.J., Letourneau, P.C., and Borisy, G.G. (1990). A test of microtubule translocation during neurite elongation. *J. Cell Biol.* 111, 123–130.
7. Okabe, S., and Hirokawa, N. (1990). Turnover of fluorescently labelled tubulin and actin in the axon. *Nature* 343, 479–482.
8. Sabry, J., O'Connor, T.P., and Kirschner, M.W. (1995). Axonal transport of tubulin in T11 pioneer neurons in situ. *Neuron* 14, 1247–1256.
9. Takeda, S., Funakoshi, T., and Hirokawa, N. (1995). Tubulin dynamics in neuronal axons of living zebrafish embryos. *Neuron* 14, 1257–1264.
10. Reinsch, S.S., Mitchison, T.J., and Kirschner, M.W. (1991). Microtubule polymer assembly and transport during axonal elongation. *J. Cell Biol.* 115, 365–379.
11. Okabe, S., and Hirokawa, N. (1992). Differential behavior of photoactivated microtubules in growing axons of mouse and frog neurons. *J. Cell Biol.* 117, 105–120.
12. Okabe, S., and Hirokawa, N. (1993). Do photobleached fluorescent microtubules move? Re-evaluation of fluorescence laser photobleaching both in vitro and in growing *Xenopus* axons. *J. Cell Biol.* 120, 1177–1186.
13. Chang, S.H., Rodionov, V.I., Borisy, G.G., and Popov, S.V. (1998). Transport and turnover of microtubules in frog neurons depend on the pattern of axonal growth. *J. Neurosci.* 18, 821–829.
14. Tanaka, E.M., and Kirschner, M.W. (1991). Microtubule behavior in the growth cones of living neurons during axon elongation. *J. Cell Biol.* 115, 345–363.
15. Dent, E.W., Callaway, J.L., Szebenyi, G., Baas, P.W., and Kail, K. (1999). Reorganization and movement of microtubules in axonal growth cones and developing interstitial branches. *J. Neurosci.* 19, 8894–8908.
16. Chang, S., Svitkina, T.M., Borisy, G.G., and Popov, S.V. (1999). Speckle microscopic evaluation of microtubule transport in growing nerve processes. *Nat. Cell Biol.* 1, 399–403.
17. Wang, L., Ho, C.-L., Sun, D., Liem, R.K.H., and Brown, A. (2000). Rapid movement of axonal neurofilaments interrupted by prolonged pauses. *Nat. Cell Biol.* 2, 137–141.
18. Roy, S., Coffee, P., Smith, G., Liem, R.K.H., Brady, S.T., and Black, M.M. (2000). Neurofilaments are transported rapidly but intermittently in axons: implications for slow axonal transport. *J. Neurosci.* 20, 6849–6861.
19. Brown, A. (2000). Slow axonal transport: stop and go traffic in the axon. *Nat. Rev. Mol. Cell Biol.* 1, 153–156.
20. Wang, L., and Brown, A. (2001). Rapid intermittent movement of axonal neurofilaments observed by fluorescence photobleaching. *Mol. Biol. Cell* 12, 3257–3267.
21. Black, M.M., Keyser, P., and Sobel, E. (1986). Interval between the synthesis and assembly of cytoskeletal proteins in cultured neurons. *J. Neurosci.* 6, 1004–1012.
22. Rodionov, V., Nadezhkina, E., and Borisy, G. (1999). Centrosomal control of microtubule dynamics. *Proc. Natl. Acad. Sci. USA* 96, 115–120.
23. Ahmad, F.J., and Baas, P.W. (1995). Microtubules released from the neuronal centrosome are transported into the axon. *J. Cell Sci.* 108, 2761–2769.
24. Black, M.M., and Lasek, R.J. (1980). Slow components of axonal transport: two cytoskeletal networks. *J. Cell Biol.* 86, 616–623.
25. Oblinger, M.M., Brady, S.T., McQuarrie, I.G., and Lasek, R.J. (1987). Cytotypic differences in the protein composition of the axonally transported cytoskeleton in mammalian neurons. *J. Neurosci.* 7, 453–462.
26. Brown, A., Li, Y., Slaughter, T., and Black, M.M. (1993). Composite microtubules of the axon: quantitative analysis of tyrosinated and acetylated tubulin along individual axonal microtubules. *J. Cell Sci.* 104, 339–352.
27. Brown, A. (1997). Visualization of single neurofilaments by immunofluorescence microscopy of splayed axonal cytoskeletons. *Cell Motil. Cytoskeleton* 38, 133–145.
28. Bray, D., and Bunge, M.B. (1981). Serial analysis of microtubules in cultured rat sensory axons. *J. Neurocytol.* 10, 589–605.
29. Ahmad, F.J., Yu, W., McNally, F.J., and Baas, P.W. (1999). An essential role for katanin in severing microtubules in the neuron. *J. Cell Biol.* 145, 305–315.
30. Ahmad, F.J., Joshi, H.C., Centonze, V.E., and Baas, P.W. (1994).

- Inhibition of microtubule nucleation at the neuronal centrosome compromises axon growth. *Neuron* 12, 271–280.
31. Yu, W., Schwei, M.J., and Baas, P.W. (1996). Microtubule transport and assembly during axon growth. *J. Cell Biol.* 133, 151–157.
 32. Slaughter, T., Wang, J., and Black, M.M. (1997). Microtubule transport from the cell body into the axons of growing neurons. *J. Neurosci.* 17, 5807–5819.
 33. Galbraith, J.A., Reese, T.S., Schlieff, M.L., and Gallant, P.E. (1999). Slow transport of unpolymerized tubulin and polymerized neurofilament in the squid giant axon. *Proc. Natl. Acad. Sci. USA* 96, 11589–11594.
 34. Terada, S., Kinjo, M., and Hirokawa, N. (2000). Oligomeric tubulin in large transporting complex is transported via kinesin in squid giant axons. *Cell* 103, 141–155.
 35. Baas, P.W. (2002). Microtubule transport in the axon. *Int. Rev. Cytol.* 212, 41–62.
 36. Susalka, S.J., and Pfister, K.K. (2000). Cytoplasmic dynein subunit heterogeneity: implications for axonal transport. *J. Neurocytol.* 29, 819–829.
 37. Ahmad, F.J., Echeverri, C.J., Vallee, R.B., and Baas, P.W. (1998). Cytoplasmic dynein and dynactin are required for the transport of microtubules into the axon. *J. Cell Biol.* 140, 391–401.
 38. Brown, A., Slaughter, T., and Black, M.M. (1992). Newly assembled microtubules are concentrated in the proximal and distal regions of growing axons. *J. Cell Biol.* 119, 867–882.